Modeling Temperature Responses of Leaf Growth, Development, and Biomass in Maize with MAIZSIM

Soo-Hyung Kim,* Yang Yang, Dennis J. Timlin, David H. Fleisher, Annette Dathe, Vangimalla R. Reddy, and Kenneth Staver

ABSTRACT

Mechanistic crop models capable of representing realistic temperature responses of key physiological processes are necessary for enhancing our ability to forecast crop yields and develop adaptive cropping solutions for achieving food security in a changing climate. Leaf growth and phenology are critical components of crop growth and yield that are sensitive to climate impacts. We developed a novel modeling approach that incorporates a set of nonlinear functions to augment traditional thermal time methods (e.g., growing degree days) for simulating temperature responses of leaf expansion and phenology in maize or corn (*Zea mays* L.). The resulting leaf expansion and phenology models have been implemented into a new crop model, MAIZSIM, that simulates crop growth based on key physiological and physical processes including C_4 photosynthesis, canopy radiative transfer, C partitioning, water relations, and N dynamics for a maize plant. Coupled with a two-dimensional soil process model, 2DSOIL, MAIZSIM was applied to simulate leaf growth, phenology, biomass partitioning, and overall growth of maize plants planted at two field sites on the Eastern Shore of Maryland and in Delaware for 3 yr of data. The model parameters were estimated using data from outdoor sunlit growth chambers and the literature. No calibration was performed using the field data. The MAIZSIM model simulated leaf area, leaf addition rate, leaf numbers, biomass partitioning and accumulation with reasonable accuracy. Our study provides a feasible method for integrating nonlinear temperature relationships into crop models that use traditional thermal time approaches without sacrificing their current structure for predicting the climate change impacts on crops.

Explanatory crop and soil simulation models are problem-solving tools that are well suited to addressing today's multiple agricultural challenges. Simulation models provide quantitative descriptions of plant and soil behavior, and calculate their responses to environmental changes, climate variability, and agricultural management. They are useful both as decision support tools for on-farm management and for assessment of agricultural policies and practices. Many existing models simulate growth and yield of a generic plant. The growth rate is a function of time (RZWQM, Ahuja et. al., 2000) or ambient temperature expressed in thermal units (APSIM, Keating et al., 2003; EPIC, Williams, 1995; CERES, Jones and Kiniry, 1986; CROPGRO, Boote et al., 1998) modified by C availability, and biomass accrues according to intercepted radiation. In most cases, different plant species are simulated utilizing appropriate parameter files, but the basic processes are the same.

Globally, corn or maize is one of the most important food crops and is the most important crop with a C_4 photosynthetic pathway; only wheat (*Triticum aestivum* L.) and rice (*Oryza sativa* L.) are ahead of maize in terms of total global production. Despite the importance of maize, relatively few simulation models have been developed for this crop. Among the most widely used models for maize are CERES-Maize (Jones and Kiniry, 1986) and EPIC (Williams, 1995). More recently, Lizaso et al. (2011) developed a new maize simulation model, CSM-IXIM, by adapting code from CERES-Maize to describe individual leaf area growth, leaf-level C assimilation and partitioning scaled to the canopy level, and growth of reproductive organs. Yang et al. (2004) also developed a maize simulation model, Hybrid-Maize, by combining components of CERES-Maize with components of INTERCOM and Wofost (van Ittersum et al., 2003).

Attempts to assess the impacts of global climate changes on maize production have been made using both CERES-Maize (Iqbal et al., 2011) and EPIC (Gaiser et al., 2011; Brown and Rosenberg, 1999). Stockle et al. (1992) modified the EPIC model to assess the impacts of elevated CO_2 concentration and associated climate changes. Both CERES-Maize and EPIC calculate biomass through radiation use efficiency parameters. Stockle et al. (1992) modified EPIC to describe an empirical link between the response of crop biomass production and crop transpiration to changes in the atmospheric CO_2 concentration and vapor pressure deficit. In order for researchers to be able to predict the climate impacts realistically, process-level models that incorporate physiological processes (e.g., canopy development, phenology, CO_2 assimilation, stomatal relations, and transpiration) on a mechanistic level are essential.

S.-H. Kim, School of Environmental and Forest Sciences, College of the Environment, Univ. of Washington, Seattle, WA 98195; Y. Yang, Dow Agrosciences, Indianapolis, IN 46268; D. Timlin, D.H. Fleisher, and V.R. Reddy, USDA-ARS Crop Systems and Global Change Lab., Beltsville, MD 20705; and A. Dathe and K. Staver, Wye Research and Education Center, Univ. of Maryland, Queenstown, MD 21658. Received 30 Sept. 2011. *Corresponding author (soohkim@uw.edu).

Published in Agron. J. 104:1523–1537 (2012)
Posted online 9 Aug. 2012
doi:10.2134/agronj2011.0321

Abbreviations: GDD, growing degree days; LTAR, leaf tip appearance rate; SPAR, Soil–Plant–Atmosphere Research.

Crop-level C assimilation depends on canopy development and the resultant green leaf area. Leaf area determines the fraction of incident photosynthetically active radiation intercepted by the crop canopy and ultimately dry matter production. Leaves are also the main path for transpiration and C assimilation. If the crop leaf area is not calculated accurately, the estimation of dry matter and yield components, as well as water use and nutrient uptake, will be incorrect. Thus, simulation of green leaf area during the growing season is a crucial component of crop growth models. In some models (e.g., ECOSYS, Grant, 1989b; GOSSYM, Baker et al., 1983; Whisler et al., 1987; CSM-CROPGRO, Jones et al., 2003; Hoogenboom et al., 2010), total plant leaf area is calculated from the biomass partitioned to the leaves, using the concept of specific leaf area. In the models proposed by Arkebauer et al. (1995) as well as Fournier and Andrieu (1998), leaf expansion and leaf senescence are driven mainly by accumulated thermal time and are simulated separately on a per-leaf basis. This methodology has been adopted in several recently developed models (Lafarge and Tardieu, 2002; Dosio et al., 2003; Lizaso et al., 2003, 2011; Yang et al., 2004; Fleisher and Timlin, 2006) for different crops such as sunflower (*Helianthus annuus* L.), potato (*Solanum tuberosum* L.), and maize. These models provide more flexible and robust approaches for leaf area simulation, but, with some exceptions (e.g., CSM-IXIM by Lizaso et al., 2011), most still do not link leaf expansion and C physiology.

A majority of simulation models use the thermal time concept of accumulated growing degree days (GDD) with a base temperature to quantify temperature effects on canopy growth and plant development. Growing degree days is a convenient and physically based method to express plant development on a temperature-weighted temporal scale. A disadvantage of the GDD concept, however, is that it is a linear scale. Although thermal time can be made to account for the negative effects of high temperature on the growth rate by incorporating a segmented "broken stick" type of relationship, it depicts the response from each segment as an additive linear relationship.

The metabolic responses of plants to temperature are not necessarily linear even during the initial increasing phase at low temperatures and have an optimum after which the rates decline steeply in a nonlinear fashion. This type of nonlinear response to temperature is found in various physiological processes and plant traits including leaf phenology (Warrington and Kanemasu, 1983b), photosynthesis (Kim et al. 2007), leaf size (Birch et al., 1998a), and leaf growth (Fleisher and Timlin, 2006). As illustrated with leaf appearance rates in potato (Fleisher et al., 2006) and maize (Birch et al., 1998b; Kim et al., 2007), phyllochrons calculated from linear GDD can be influenced substantially by growth temperatures, especially under high temperatures. That is, phyllochron values determined using GDD could vary considerably for the same crop if grown under high or low temperatures beyond the optimal (Bollero et al., 1996; Kim et al., 2007) or if grown in regions that have similar mean daily temperatures but different daily temperature extremes (Birch et al., 1998b; Loomis and Connor, 1996).

Incorporation of a nonlinear temperature response function in a crop model is critical when simulating crop responses under an environment where temperature fluctuation is large near the inflection point, a rapidly increasing or decreasing region, or an optimal region of the temperature response of the crop. Realistic representation of the nonlinear temperature response of crop development is important for predictions of the impacts of extreme temperatures on crop production. The importance and necessity of implementing nonlinear temperature responses to crop models for predicting climate impacts on crop yield have been highlighted using historical maize yield data in Africa by Lobell et al. (2011). They illustrated the need for new approaches in crop models that explicitly account for supraoptimal temperature effects to enhance our understanding of climate impacts on crop yields, particularly in tropical regions (Lobell et al., 2011).

Several attempts have been made to overcome the shortcomings of the linear thermal time concept by using various types of equations including bilinear, exponential, Arrhenius, polynomial, and β distribution models (Hesketh and Warrington 1989; Stewart et al., 1998; Yin et al., 2003; Yin and Kropff, 1996). For its flexibility, simplicity, and intuitiveness, the β distribution model is a promising alternative to thermal time models (Yin et al., 1995). Yin et al. (1995) demonstrated that the β function performed well against two widely used thermal time approaches.

Converting the information expressed in GDD to developmental rates used in nonlinear models such as the β function can be done using algebra and statistical methods without fitting new parameters to additional experimental data.

The objective of this study was to augment the traditional thermal time approach for the calculation of leaf area expansion and phenology by coupling nonlinear rate equations with the GDD-based models and to link leaf area expansion with C physiology for biomass accumulation and partitioning. The equations for this new approach are implemented in the new maize simulation model MAIZSIM (Yang et al., 2009a, 2009b). The MAIZSIM model calculates leaf initiation and expansion, light interception, photosynthesis, C and N partitioning, root and canopy growth, phenology, root growth, and water and N uptake. The crop model is interfaced with the soil model 2DSOIL (Timlin et al., 1996) for the belowground components.

MATERIALS AND METHODS

Model Description

The computer program for the maize model in MAIZSIM has a modular design that follows the object-oriented design for crop models described by Acock and Reynolds (1997), Reynolds and Acock (1997), and Acock and Reddy (1997). The components were developed from existing paradigms and modified specifically for maize. The crop model is coupled with the modular soil process model 2DSOIL (Timlin et al., 1996). In the coupled model, the crop component of MAIZSIM simulates maize growth and development as a function of light, temperature, humidity, CO_2, N, water status, and soil properties. The 2DSOIL model has a two-dimensional, finite-element representation of the soil profile and simulates heat and water movement and solute transport. The 2DSOIL model also estimates evapotranspiration and heat flux at the soil surface (Timlin et al., 2002), as well as root growth as taken from GLYCIM (Acock et al., 1982). Coupling a crop model with 2DSOIL provides a soil–plant–atmosphere continuum system that has the potential for taking into account information on the dynamic

soil water status in simulating crop growth and development (Yang et al., 2009a, 2009b). Leaf and reproductive organ development rates in MAIZSIM are driven by current hourly ambient temperature and not by accumulated thermal time (GDD). The soil model 2DSOIL is written in FORTRAN, while the crop model is coded in C++ and is linked as a subroutine within 2DSOIL.

The MAIZSIM model simulates the growth of individual leaves rather than the entire canopy (as a "big leaf"). Leaf growth consists of four processes: initiation, appearance, expansion, and senescence. As a maize plant develops, leaf initiation occurs within the whorl, and new leaves are not visible without dissecting the plant. Knowledge of leaf initiation is important, however, because it indicates the phenological development of the plant, and the leaf initiation and growth rates are dependent on current environmental conditions. The leaf appearance rate applies to the appearance of leaf tips within the whorl, which are visible to an observer. After leaf initiation and appearance, leaf expansion and senescence are simulated on an individual-leaf basis.

Simulation of Maize Leaf Initiation and Appearance

A simplified β function (Yan and Hunt, 1999) used to calculate temperature-dependent [$r(T)$] processes in MAIZSIM is represented by the following empirical equation:

$$r(T) = R_{\max}\left(\frac{T_{\text{ceil}} - T}{T_{\text{ceil}} - T_{\text{opt}}}\right)\left(\frac{T}{T_{\text{opt}}}\right)^{T_{\text{opt}}/(T_{\text{ceil}} - T_{\text{opt}})} \quad [1]$$

where the temperature-dependent rate of development is represented by $r(T)$, T is the mean hourly ambient air temperature as an input variable, T_{opt} is the optimal temperature at which the maximal rate of development [$r(T) = R_{\max}$] occurs, and T_{ceil} is the ceiling temperature at which development ceases [$r(T) = 0$]. This equation assumes that the base (or minimal) temperature is zero, although other base temperatures can be used. Yan and Hunt (1999) showed that T_{opt} and T_{ceil} were similar among different developmental events in maize. The simplified β function (Eq. [1]) is used in MAIZSIM to calculate the rates of seedling emergence, primordia initiation, tip and ligule appearance, and leaf area expansion as a function of current temperature (Fig. 1 and 2). Soil surface temperature is used until the tip of the eighth leaf appears, after which current ambient 2-m air temperature is used.

Simulation of Leaf Expansion

The hourly rate of increase for the area of a single leaf is calculated using Lizaso et al. (2003, Eq. [3]). This is the first derivative with respect to time of a logistic equation for the area of a single leaf (Lizaso et al., 2003, Eq. [2]):

$$\frac{dA_i}{dt} = (\text{Ae}_i \text{ke}_i) \times \frac{\exp\left[-\text{ke}_i(t - \text{te}_i)\right]}{\left\{1 + \exp\left[-\text{ke}_i(t - \text{te}_i)\right]\right\}^2} f(T) \quad [2]$$

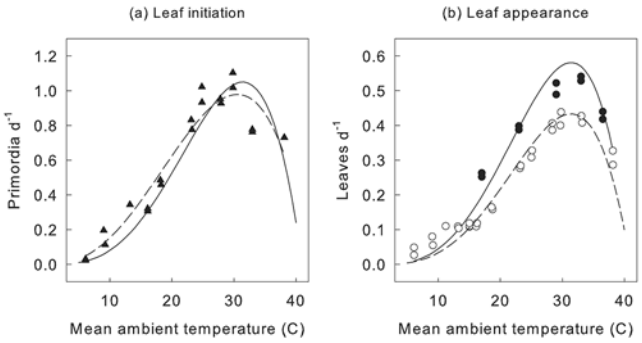

Fig. 1. Leaf initiation and appearance rates as a function of daily mean ambient temperature: (A) leaf initiation rate for observations (▲) from Warrington and Kanemasu (1983b), with solid line representing predictions of the model using parameter values from this study and dashed line representing the best fit of Eq. [1] with all three parameters fitted with observations; and (B) leaf tip and ligule appearance rate for observations of leaf tip appearance (●) from the Soil–Plant–Atmosphere Research (SPAR) chamber experiment and observations of ligule appearance (○) from Warrington and Kanemasu (1983b), with solid and dashed lines representing model predictions for tip and ligule, respectively, using parameter values from this study.

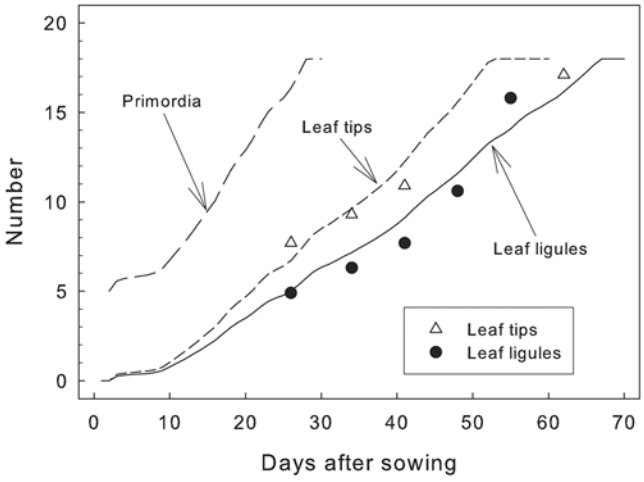

Fig. 2. Simulation of leaf initiation, tip appearance, and ligule appearance. Symbols represent observations from the field experiment; long-dashed, short-dashed, and solid lines represent predicted rates of primordia initiation, tip appearance, and ligule appearance of leaves, respectively. Primordia were estimated only because they could not be nondestructively measured.

where Ae_i is the potential fully expanded surface area (cm^2) of the ith leaf, te_i is the thermal time (GDD after emergence, base 8°C) when the leaf reaches 50% of its final area, and ke_i is a unitless parameter controlling the slope of the curve or growth rate. A nonlinear temperature function, $f(T)$, is used to scale the effect of growth temperatures on the leaf expansion rate. This function is described in full detail below (see Eq. [14]). The value of Ae_i is calculated using a modification of the relationship proposed by Dwyer et al. (1992). This modification was used by both Lizaso et al. (2003) and Fournier and Andrieu (1998). We applied the implementation of Fournier and Andrieu (1998) because they gave explicit equations for the parameters. Note that the parameters vary by leaf rank (i):

$$\mathrm{Ae}_i = \mathrm{Ae}_\mathrm{m} \exp\left[a\left(\frac{\mathrm{NL}_i}{N_\mathrm{m}} - 1\right)^2 + b\left(\frac{\mathrm{NL}_i}{N_\mathrm{m}} - 1\right)^3\right] \quad [3]$$

where Ae_i and NL_i are the area and rank, respectively, of the ith leaf; Ae_m and N_m are the area and rank, respectively, of the largest leaf on the plant, and a and b are parameters. The final surface area of the largest leaf will probably vary with genotype and environment. We assumed that the data reported in the literature for Ae_m or other parameters used to determine Ae_m (see below) represent the potential values obtained at or near optimal growth conditions (e.g., Fournier and Andrieu, 1998; Lizaso et al., 2003). Based on data compiled from the literature, Fournier and Andrieu (1998) gave these equations for the rank of the largest leaf, N_m, and for a and b in Eq. [3] as a function of the total number of leaves (N_t):

$$N_\mathrm{m} = 5.93 + 0.33N_\mathrm{t} \quad [4]$$

$$a = -10.61 + 0.25N_\mathrm{t} \quad [5]$$

$$b = -5.99 + 0.27N_\mathrm{t} \quad [6]$$

and Ae_m was calculated as (Fournier and Andrieu, 1998; Francis et al., 1969; Birch et al., 1998a)

$$\mathrm{Ae}_\mathrm{m} = L_\mathrm{M} 0.75 W_\mathrm{max} \exp\left(-1.17 + 0.047N_\mathrm{t}\right) \quad [7]$$

where

$$L_\mathrm{M} = \sqrt{L^2_{\mathrm{M\_min}} + k\left(N_\mathrm{t} - N_\mathrm{g}\right)} \quad [8]$$

and

$$W_\mathrm{max} = 0.106L_\mathrm{M} \quad [9]$$

where L_M is the length of the largest leaf of a plant, $L_{\mathrm{M\_min}}$ is a length characteristic of the largest leaf of a cultivar when grown to develop the minimal (i.e., generic) total leaf number (N_g), k is a parameter (k = 24 cm^2), N_t is the actual number of total leaves, and N_g is the generic minimal number of total leaves, which is a hybrid characteristic. This number is found when the plant is grown under certain temperature and photoperiod conditions that minimize additional development of leaf primordia before tassel initiation (Warrington and Kanemasu, 1983b; Grant 1989a). We applied an $L_{\mathrm{M\_min}}$ (length) value of 115 cm to scale the potential area of the largest leaf (Ae_m, Eq. [7]) grown at optimal temperatures (T_pk, see Eq. [14] below) to 1057 cm^2 when N_t and N_g are at 25 leaves using the leaf number vs. largest leaf area relationship (Eq. [7]) described by Birch et al. (1998a). This relationship (Eq. [7] and [8]) scales the potential area of the largest leaf based on N_t as well as the difference between N_t and N_g, resulting in a value between 750 and 800 cm^2 when N_t = 18 or 19 and N_g = 16 or 17. These values match the reported values of several cultivars at multiple locations (Muchow et al., 1990). On initialization, N_t is set as N_g but can change depending on the time it takes the plant to reach the reproductive stage after accounting for the effect of photoperiod and temperature on the final leaf number, as used by Grant (1989a). The area of the individual ith leaf is calculated in Eq. [3]. The interpretation of Eq. [3] is that the area of a leaf at any node is scaled to the area of the largest leaf as a function of the position of the leaf on the plant. The leaf area of an individual leaf is defined by a characteristic length of the largest leaf and the number of leaves (Eq. [4–9]). This equation (Eq. [3]) reproduces a bell-shaped distribution of leaves (Fournier and Andrieu, 1998).

The leaf expansion rate relative to the potential leaf area was calculated using Eq. [2]. We assumed that the parameters in Eq. [2] (Ae_i, ke_i, and te_i) from Lizaso et al. (2003) were also determined at or near optimal growing conditions. These parameters were calculated by Lizaso et al. (2003) as

$$\mathrm{ke}_{i\_\mathrm{max}} = k_\mathrm{o} + k_x \exp\left[-\frac{\left(\mathrm{LN}_i - 1\right)^2}{2W_k^2}\right] \quad [10]$$

where $\mathrm{ke}_{i\_\mathrm{max}}$ is the potential ke_i measured under optimal temperature conditions for leaf expansion, k_o (= 0.026) is the lower asymptote of the Gaussian curve, and k_x (= 0.174) is the amplitude with respect to k_o (Lizaso et al., 2003). The parameter W_k controls the width of the curve at half the amplitude and is a function of the total number of leaves (N_t), $W_k = N_\mathrm{t}/8.18$. The same temperature relationship was assumed for te, the thermal time it takes a leaf to reach 50% of its final area:

$$\begin{aligned} \mathrm{te}_i &= \mathrm{tt}_i + \frac{2.197}{\mathrm{ke}_{i\_\mathrm{max}}} h(T) && \mathrm{rank} > 2 \\ \mathrm{te}_i &= 25\mathrm{LN}_i && \mathrm{rank} \le 2 \end{aligned} \quad [11]$$

where tt_i and te_i are thermal time after emergence (GDD_8C), $\mathrm{ke}_{i\_\mathrm{max}}$ is from Eq. [10], and i refers to the leaf number. The parameter te_i responds to temperature through tt_i and $h(T)$; these are described in detail below (see Eq. [12] and [16]). The thermal time from emergence to tip appearance of the ith leaf (tt_i) is calculated as (Lizaso et al., 2003)

$$\mathrm{tt}_i = \left(\mathrm{LN}_i - 2\right)\mathrm{PHY} + \mathrm{tt}_2 \quad [12]$$

where LN_i is the nodal position of the ith leaf (LN > 2), PHY is the phyllochron (GDD needed before a new leaf emerges with a base temperature of 8°C), and tt_2 is the thermal time from emergence to the appearance of the second leaf. The parameter PHY used by Lizaso et al. (2003) is hybrid specific and is calibrated from observed data; PHY (based on air temperature) can be related to the β function parameters for leaf tip appearance by

$$\mathrm{PHY} = \left(\frac{T_\mathrm{opt} - T_\mathrm{b}}{R_{\mathrm{max\_LTAR}}}\right) \quad [13]$$

where T_opt is the optimal air temperature for the leaf tip appearance rate (32.1°C) (Kim et al., 2007) and T_b is the base temperature for calculating growing degree days (GDD_8C) used in the leaf growth and development functions. Thus, this equation

Table 1. Values for temperature-dependence parameters used in leaf addition and expansion.

Parameter	Equation	Value	Description
			Leaf initiation and appearance
T_{opt}, °C	[1], [13]	30.5, 32.1	optimum temperature for leaf initiation and appearance, respectively
T_{ceil}, °C	[1]	42.7, 43.7	ceiling temperature for leaf initiation and appearance, respectively
R_{max_LTIR}, leaves d^{-1}	[1]	0.978	fit to Eq. [1], used to calculate R_{LTIR} (leaf tip initiation rate) as a function of temperature in Eq. [1]
R_{max_LTAR}, leaves d^{-1}	[1], [13]	0.53	fit to Eq. [1], used to calculate R_{LTAR} (leaf tip appearance rate) as a function of temperature in Eq. [1]
			Temperature dependence of relative leaf expansion
T_{pk}, °C	[14]	18.7	temperature at which potential leaf area is maximized
T_{opt_ke}, °C	[15], [16]	18.8	optimum temperature for leaf expansion for intrinsic leaf growth rate (ke)
T_{ceil_ke}, °C	[15]	42.7	ceiling temperature for leaf expansion
Q_{10}	[16]	1.455	temperature adjustment for growing degree days needed for a leaf to reach 50% of its fully expanded area

scales the leaf tip appearance rate (r_{LTAR})—a function of ambient air temperature (Eq. [1])—into phyllochrons (PHY) based on the observed $R_{max–LTAR}$ (maximum LTAR at T_{opt}, d^{-1}) (Table 1). This relationship also allows for backward conversion of PHY into R_{max_LTAR} if PHY is determined empirically from plants grown in temperatures between T_b and T_{opt}.

Leaf longevity (based on GDD_{8C}) is calculated as in Lizaso et al. (2003, Eq. [10]– [12]). Leaf senescence is considered to be a negative growth, resulting in a decrease in the current leaf area. It is calculated as in Lizaso et al. (2003) using an equation similar to Eq. [2], where Ae_m is the actual area of the largest leaf (phenotypic) rather than its potential area (genotypic). The parameter ke for senescence is calculated as in Eq. [10], where $k_o = 0.1$ and $k_x = 0.02$, through Eq. [13]. The rate for leaf senescence is about half that for growth. The original parameters and equations were retained for this relationship. There were no temperature adjustments.

Nonlinear Temperature Dependence of Leaf Expansion Parameters

The calculation of individual leaf area expansion and development is based on equations given by Lizaso et al. (2003) and Fournier and Andrieu (1998), as described above. These models assume that the linear relationship between leaf growth and GDD requirements remain unchanged throughout a range of temperatures, even at high or low temperatures where cell expansion is likely to slow down. We augmented these GDD-based approaches to be capable of representing temperature responses using nonlinear temperature relationships. Nonlinear temperature dependence of plant leaf area (Bos et al., 2000; Kim et al., 2007; Tollenaar, 1989) as well as individual leaf size (Fournier and Andrieu, 1998; Hesketh and Warrington, 1989) have been demonstrated in previous studies. Earlier studies (e.g., Daughtry and Hollinger, 1984; Francis et al., 1969; Pearce et al., 1975) have established consistent linear relationships between individual leaf area and total plant leaf area. Therefore, we pooled both whole-plant and individual leaf area data from the literature to model the nonlinear temperature response of leaf size using a peaked exponential function:

$$f(T) = \max\left[0.0, \frac{T - T_b}{T_{pk}} \exp\left(1.0 - \frac{T - T_b}{T_{pk}}\right)\right] \quad [14]$$

where T is the air temperature and T_{pk} is the peak temperature at which this function [$f(T)$] reaches the maximum value (= 1.0) (Table 1). In our model, $f(T)$ scales hourly leaf expansion (Eq. [2]) in proportion to the potential final leaf size at rank i (Ae_i) as a function of the current growth temperature. Starting from zero at T_b, this function rapidly rises to reach the maximum at T_{pk}, then gradually declines with increasing temperature (Fig. 3a). The same base temperature (T_b) of 8°C was applied in this study. The peak temperature (T_{pk}) of 18.7°C was determined based on reported data in the literature for whole-plant leaf area (Bos et al., 2000; Kim et al., 2007; Tollenaar, 1989) as well as individual leaf size (Fournier and Andrieu, 1998; Hesketh and Warrington, 1989). These data were digitized and normalized using ImageJ software (National Institutes of Health) so that the maximum values are centered around 1.0. This function describes no leaf expansion at or below 8°C.

The temperature dependence of the intrinsic growth rate parameter, ke_i, was modeled using a reduced β function (Yan and Hunt, 1999) in response to air temperature as

$$ke_i = ke_{i\_max}\left(\frac{T_{ceil\_ke} - T}{T_{ceil\_ke} - T_{opt\_ke}}\right) \times \left(\frac{T}{T_{opt\_ke}}\right)^{T_{opt\_ke}/(T_{ceil\_ke} - T_{opt\_ke})} \quad [15]$$

where T_{opt_ke} is the optimal temperature at which the maximal intrinsic growth rate ($ke_i = ke_{i–max}$) is achieved and T_{ceil_ke} is the ceiling temperature at which leaf growth ceases ($ke_i = 0$) (Table 1; Fig. 3b).

Similarly, the temperature dependence of GDD required for 50% leaf expansion (te) defined in Eq. [11] is adjusted in response to air temperature by $h(T)$ (Fig. 3b):

$$h(T) = Q_{10}^{\left[(T - T_{opt\_ke})/10\right]} \quad [16]$$

where Q_{10} is a parameter that controls the rate of change in te with temperature. This function is scaled to 1.0 when the air temperature (T) is equal to T_{opt_ke}, which is the optimum temperature at which the $ke_{i–max}$ is observed (Table 1).

Parameter values for Eq. [15] and [16] were estimated using whole-plant leaf area data from growth chamber experiments performed under multiple day/night temperature combinations

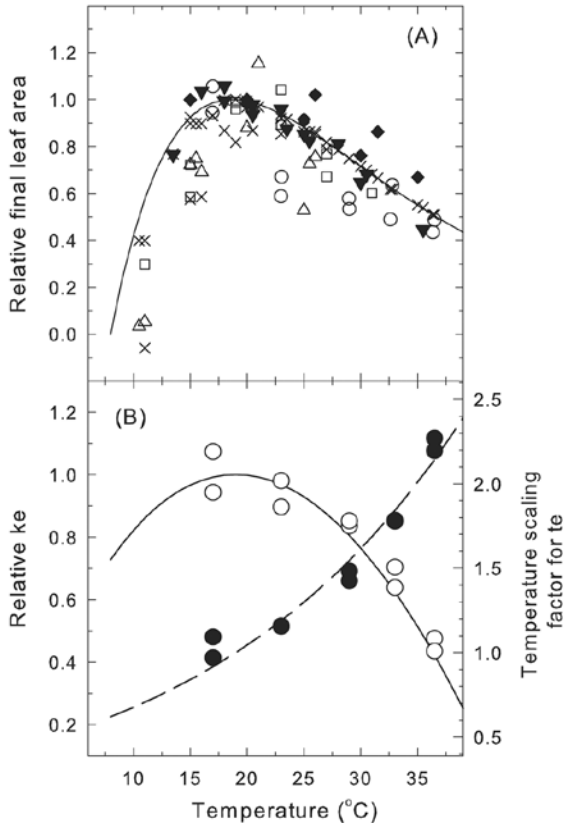

Fig. 3. Temperature dependence of relative final leaf area (Ae), intrinsic leaf growth rate (ke), and the inflection point at which 50% leaf expansion occurs (te) in the leaf growth model as described in Eq. [2]: (A) relative final leaf area as a function of growth temperature (Eq. [14]), with symbols representing relative Ae reported in the literature for whole plant (○, Kim et al., 2007; △, Bos et al., 2000; □, Tollenaar, 1989) or individual leaves (▼ Hesketh and Warrington, 1989; ◆ Fournier and Andrieu, 1998); model predictions accounting for day/night temperature differences (×) and using daily mean temperatures (solid line) are also shown; and (B) relative ke (○) and temperature scaling factor for te (●) from Kim et al. (2007) compared with model ke (solid line) and modeled scaling factor for te (dashed line) described in Eq. [15] and [16].

(Kim et al., 2007). We used an integral form of Eq. [2] from Kim et al. (2007) to estimate ke and te as functions of temperature for the experimental data:

$$Ae_j = \frac{Ae_{m,j}}{1+\exp\left[-ke_j\left(t-te_j\right)\right]} \qquad [17]$$

where Ae_j is the plant leaf area (cm^2) at thermal time (GDD_{8C}) t for temperature treatment j, $Ae_{m,j}$ is the final, end-of-season, whole-plant leaf area (cm^2 $plant^{-1}$) for temperature treatment j, te_j is the thermal time (GDD_{8C} after emergence) when the plant leaf area reaches 50% of its final area, and ke_j is the growth rate (GDD^{-1}) for temperature treatment j. The estimated values of ke_j and te_j for each temperature treatment were combined and their temperature dependence determined by fitting with Eq. [15–17] using Proc NLIN in SAS/STAT software (Version 9.3 of SAS for Windows (SAS Institute). This process enabled us to characterize the nonlinear dependence of three leaf expansion parameters (Ae, te, and ke) used by Lizaso et al. (2003) on air temperatures and to augment the leaf expansion model as a function of GDD with a nonlinear temperature response. Leaf size increment at each time step (i.e., dAe_i/dt in Eq. [2]) was adjusted to respond to hourly growth temperature by multiplying a peaked exponential function (Eq. [14]) by the potential leaf size (Ae_i) achievable for the temperature. Both ke_i and te_i were also adjusted to respond to hourly growth temperature using Eq. [15] and [16], respectively. Temperature-dependent parameters for leaf phenology and expansion estimated in this study are listed in Table 1. The parameters for leaf senescence were not adjusted to respond to hourly air temperature.

Simulation of Maize Phenological Development and Carbon Partitioning

Tassel initiation, anthesis, and total number of leaves were modeled as a function of ambient hourly temperature and photoperiod based on Grant (1989a). The governing temperature-dependent rate parameters for the equations were determined from the hourly air temperature using a β function (Eq. [1]). The number of leaf primordia just before the inductive phase (i.e., minimum number of leaves without additions due to temperature or photoperiod: L_{min}) was defined as a cultivar-specific coefficient (Grant 1989a). Parameter values of Eq. [1] for calculation of the leaf initiation rate (r_{LIR}) or leaf tip appearance rate (r_{LTAR}) as a function of temperature were estimated using SAS/STAT Proc NLIN. Primordia of five leaves were assumed to be present in the embryo of a seed. The values of R_{max_LIR}, T_{LIR_opt}, and T_{LIR_ceil} for the leaf initiation rate were calibrated with data from the literature (e.g., Warrington and Kanemasu 1983a; Yan and Hunt, 1999). The corresponding parameters for leaf tip appearance rate (e.g., R_{max_LTAR}, T_{LTAR_opt}, and T_{LTAR_ceil}) were calibrated using plant leaf area data at five different combinations of day/night temperatures under ambient CO_2 concentrations for maize plants grown in Soil–Plant–Atmosphere Research (SPAR) sunlit growth chambers described in Kim et al. (2007).

Potential, unstressed, leaf area growth is driven by temperature and then modified by C and water availability as described above and by Yang et al. (2009b). Total C is partitioned to the leaf, stem, ear, and root classes according to the methods of Grant (1989b). We did not use specific leaf area as an input variable because it is highly dependent on the environment (Tardieu et al., 1999). Specific leaf area is an emergent property of the simulation in our model. Carbon is partitioned to the individual leaves according to the relative growth rate among all growing leaves. In the case of the stem and roots, the C demand is equal to the new stem or root mass multiplied by the fraction of dry matter that is C. If there is not enough C to support all growth, the growth is limited proportionately. Additional C can be diverted to root growth in the case of water stress, as is done in GLYCIM (Acock et al., 1982). Partitioning of C to reproductive growth is modeled using phenological growth stages and empirical equations from Grant (1989b). All C is partitioned to reproductive growth after the reproductive stage (temperature function) is reached. All parameters used for phenology and C partitioning came from Grant (1989a, 1989b).

Simulation of Carbon Assimilation and Transpiration

Photosynthesis is simulated using a biochemical model of C_4 photosynthesis (von Caemmerer, 2000) coupled with a stomatal conductance model (Ball et al., 1987) and energy balance model. A full description of the coupling process can be found in Kim and Lieth (2003). The C_4 photosynthesis model was parameterized with maize leaf gas exchange data obtained using a portable photosynthesis system (LI-COR LI-6400). Full experimental details were provided by Kim et al. (2006, 2007). The temperature dependence of the C_4 photosynthesis model was implemented as described in Kim et al. (2007). The effect of water status on stomatal conductance is modeled using a function of soil water and leaf water potentials (Yang et al., 2009a; Tuzet et al., 2003). Leaf-level photosynthesis is scaled to the plant level by applying the sunlit and shaded leaf approach (Campbell and Norman, 1998, p. 247–281; Lizaso et al., 2003, 2005; De Pury and Farquhar, 1997). Respiration is calculated on a mass basis as given in Amthor (2000). A hedgerow model is used to partition light between the soil and the canopy and to calculate incident radiation (Boote and Pickering, 1994; Acock et al., 1982).

Root growth is modeled similar to the approach used in GOSSYM (Baker et al., 1983) and GLYCIM (Acock et al., 1982; Lambert and Baker, 1984). The potential root growth rate in a soil cell (finite element) is a function of current root mass. Actual growth is a function of available C and constraints due to soil temperature, soil strength, and O_2 content. Water uptake is driven by leaf water and soil water potentials and the conductance of the plant–soil continuum (Cowan, 1965).

The model requires as input hourly or higher frequency values of total solar radiant energy (MJ), ambient temperature (°C), precipitation (mm), relative humidity (%), and latitude and longitude (to calculate day length and sun angle). Required soils data include soil texture, bulk density (g cm^{-3}), saturated hydraulic conductivity (cm d^{-1}), and water retention curve parameters (van Genuchten, 1980). The current version requires two hybrid-specific parameters: the generic minimal number of leaves at maturity (N_g) and the GDD_{8C} (converted from GDD_{10C} provided by seed companies) needed to reach maturity. These values are normally available in standard hybrid data from seed companies. The hybrid and other parameter estimates specific to MAIZSIM are listed in Table 2.

Experimental Data

Data to develop and test the leaf growth model, leaf gas-exchange model, and crop development model were obtained from a set of experiments performed in sunlit SPAR growth chambers at the USDA-ARS Henry A. Wallace Agricultural Research Center (BARC) in Beltsville, MD (Kim et al., 2006, 2007). Pioneer hybrid 3733 maize plants were grown in the SPAR units at 370 or 750 μmol L^{-1} CO_2 with 19/13, 25/19, 31/25, 35/29, or 38.5/32.5°C day/night temperatures from June to October 2002. The day temperature was maintained for 16 h and the night temperature for 8 h. Additional data were obtained from a field experiment where the same maize hybrid was grown at the USDA-ARS BARC experimental farm from May to October 2002. Nitrogen was applied at the rate of 200 N kg ha^{-1} in the field experiment. In both SPAR and field experiments, leaf tip and ligule appearance rates were investigated weekly or biweekly during the vegetative stage. Leaf area and biomass were destructively measured at multiple times during the growth period. The SPAR chamber data from Kim et al. (2006, 2007) were used to calibrate the leaf growth model, leaf tip appearance rate function, and leaf gas-exchange model. The parameters in Eq. [1] and [14–17] were fit using SAS/STAT Proc NLIN and the data from the SPAR experiment (Kim et al., 2007).

Table 2. Maize hybrids planted in the field sites in Georgetown, DE, and Wye, MD and in Soil–Plant–Atmosphere Research (SPAR) chambers. All hybrids were from Pioneer.

			Growing degree days (GDD) to maturity†		
Year	Site	Hybrid	Base 50°F (GDD_{50F})‡	Base 8°C (GDD_{8C})	Min. no. of leaves
2006	Delaware	PI33B53	2700	1800	18
	Maryland	PI34M91	2630	1753	18
2007	Delaware	PI33B53	2700	1800	18
	Maryland	PI34M91	2630	1753	18
2008	Maryland	P37Y14	2400	1600	16
2002	SPAR chambers	PI3733	2400	1600	16

† Provided by Pioneer.

‡ Calculated as °F, base temperature 10°C (50°F).

Additional data for testing the model were collected from two commercial fields in Georgetown, DE, in 2006 and 2007 and two research fields at the University of Maryland's Wye Agricultural Research Center in Queenstown, MD, in 2006, 2007, and 2008. The soils in Maryland are classified as Mattapex silt loam (a fine-silty, mixed, active, mesic Aquic Hapludult) and Whitemarsh silt loam (a fine-silty, mixed, active, mesic Typic Albaquult). The soils in Delaware are classified as Pepperbox–Rosedale (loamy sand) complex (loamy, mixed, semiactive, mesic Aquic Arenic Paleudults and Arenic Hapludults) and Glassboro sandy loam (a coarse-loamy, siliceous, semiactive, mesic Aeric Endoaquult). The previous crop in Delaware was soybean [*Glycine max* (L.) Merr.]. In 2006, Pioneer hybrid 33B53 was planted on 10 April, with a row spacing of 0.76 m and population density of 7.3 plants m^{-2}. In 2007, Pioneer hybrid 33B53 was planted on 30 April at the same density. In total, ~238 kg N ha^{-1} was applied during the growing season with irrigation water both years. At the Wye Research Center, Maryland (38.91° N, 76.15° W), the previous crop was maize. Pioneer hybrid 34M91 was planted in 2006 and 2007. Pioneer hybrid 37Y14 was planted in 2008. Planting took place on 9 May 2006, 14 May 2007, and 6 June 2008. Plants in these fields were not irrigated, and 120 kg N ha^{-1} was applied in 2006 and 130 kg N ha^{-1} of N fertilizer was applied in 2007 and 2008. Plant population was 6.9 plants m^{-3}. Weather stations were set up to collect hourly data on irradiance, precipitation, ambient temperature, relative humidity, and wind run during the growth seasons at each site. Data for the hybrids used for the different sites are summarized in Table 2.

Destructive harvests were performed biweekly at the Delaware and Maryland sites. Five plants were randomly selected and destructively harvested within a 2-m row section at three different spots in each field or treatment replicate. At each location (Delaware and Maryland), five samples were taken from

each of two fields at three sites in each field. The sampled plants were separated into leaf, stem, and ear components. Dead leaves (<50% green) were separated from green leaves. Green leaf area was measured with a LI-COR LI-3100 leaf area meter, and all plant parts were dried at 60°C for 72 h and then weighed.

Performance Evaluation

To evaluate the deviation of the leaf area and biomass simulations, statistics of mean error or bias (ME), root mean square error (RMSE), model efficiency (EF), as well as Willmott's index of agreement (d) were calculated:

$$\mathrm{ME} = \frac{\sum_1^N (y_i - Y_i)}{N} \quad [18]$$

$$\mathrm{RMSE} = \sqrt{\frac{\sum_1^N (y_i - Y_i)^2}{N}} \quad [19]$$

$$\mathrm{EF} = 1 - \frac{\sum_1^N (y_i - Y)^2}{\sum_1^N (y_i - \bar{y})^2} \quad [20]$$

$$d = 1 - \frac{\sum_1^N (y_i - Y_i)^2}{\sum_1^N \left(|Y_i - \bar{y}| + |y_i - \bar{y}|\right)^2} \quad [21]$$

where y_i is the observed value, Y_i is the simulated value, and $\bar{y}$ is the mean of the observed data in a site year (appropriate to the calculation of d). The EF is a measure of the deviation between model output and the observed values relative to the scattering of the measured data. The value of EF will be 1 if simulated values match the observed values perfectly. The d value varies from 0.0 (poor model) to 1.0 (perfect model) (Willmott, 1981; Willmott et al., 1985). Plot means were used for values of y_i in the calculations rather than location means. The values were calculated using SAS/STAT Proc SQL.

RESULTS

The simplified β function described well the observed patterns of the temperature responses of leaf appearance from the SPAR chambers (Fig. 1). Because the results by Yan and Hunt (1999) suggested that the estimates of T_{opt} and T_{ceil} were similar for various developmental events, fixed values of T_{opt} and T_{ceil} were initially used to minimize the number of parameters to be calibrated. This attempt, however, underestimated the leaf initiation rate when daily mean air temperatures were <25°C (Fig. 1a). The best fit of Eq. [1] to the observed leaf initiation rates resulted in T_{opt} = 30.5°C and T_{ceil} = 42.7°C, with a somewhat lower R_{max} estimated to be 0.978 leaves d^{-1} (Fig. 1a, dashed line). Initiation of leaf primordia is a key developmental event from which other developmental events and growth rates can be derived. The best fit of Eq. [1] to leaf tip appearance rates from the SPAR chamber experiment in the ambient CO_2 concentration treatment yielded estimates of T_{opt} = 32.1°C, T_{ceil} = 43.7°C, and R_{max} = 0.53 leaves d^{-1} as described by Kim et al. (2007). The value of the maximum leaf tip appearance rate ($R_{max–LTAR}$) from the SPAR experiment was similar to that published by Yan and Hunt (1999) (0.581 leaves d^{-1}). The optimum and ceiling temperatures were also similar to the findings of Yan and Hunt (1999), Hesketh and Warrington (1989), and Warrington and Kanemasu (1983b). The rates of leaf tip and ligule appearance from the Beltsville field experiment in 2002 compared well with the model predictions made using the parameter estimates determined from the SPAR chamber experiment (Fig. 2).

Plant or individual leaf area (Ae_i), the intrinsic rate of leaf expansion (ke_i), and the inflection point (i.e., time to reach 50% expansion, te_i) fit using Eq. [14–17] shows strong nonlinear temperature dependence (Fig. 3a and 3b). The relationship in Fig. 3a, which combines data from multiple studies, shows that the relative maximum leaf area occurs at a peak temperature (T_{pk}) of 18.7°C (Reid et al. [1990] showed similar results). As temperature increased past the peak, leaf area gradually declined. The temperature dependence for the leaf expansion rate (ke_i) was fit to a reduced β function (Eq. [15]). The cardinal temperature estimates were 18.8 and 42.7°C for T_{opt_ke} and T_{ceil_ke}, respectively. Note that the estimates of optimum temperature for the maximum leaf area (T_{pk} = 18.7°C) and the temperature for the maximum growth rate (T_{opt_ke} = 18.8°C) are very close to each other. The parameter estimate for Q_{10} in Eq. [16] was 1.46 (dimensionless). This means that the thermal units required to reach 50% leaf expansion (te_i) are 1.46 times more, for example, at 35°C than at 25°C growth temperature. Taken together, these results suggest that the three parameters (Ae_i, ke_i, and te_i) used in the logistic leaf growth model (Eq. [2] and [17]) exhibit nonlinear temperature responses despite the fact that the thermal units (GDD_{8C}) are used as a driving variable (Fig. 3).

Leaf tip appearance for the Maryland and Delaware field data was approximated closely, while the total number of leaves was under- or overestimated by one leaf in some cases (Fig. 4). The data for observed leaf tips in the field at the completion of the vegetative phase ranged from 18 to 20; the simulated value also ranged from 18 to 20. The simulated rate at which the leaves appear (slopes of the rising parts of the figures) is close to the observed rates. There does not appear to be any consistent pattern in the errors due to location or planting date. The leaf tip appearance rate is rather conservative in maize and may not have a wide variance among cultivars (Warrington and Kanemasu, 1983b). All the cultivars used in the study came from one seed company (Pioneer) and all but one had similar maturity values (Table 2), probably contributing to the uniformity. The hybrid used at Maryland for 2008 was a short-season hybrid and the error was similar to that of the others. Warrington and Kanemasu (1983b) noted that leaf appearance accelerated slightly after the 12th leaf in maize, while the leaf initiation rate was constant. They attributed the increased leaf appearance rate to more rapid stem elongation and smaller leaves as the plant reached the floral initiation stage. In our field experiments, planting dates varied by 30 d or more, but that did not yield any consistent bias in the simulation results. Our results show that parameters such as leaf tip appearance rate developed from growth chamber data can be utilized under field conditions, reducing the need for field parameterization. We found similar results for potato (Fleisher et al., 2006).

The simulated increase in leaf area (Fig. 5) with time and the maximum leaf area at the field sites were very close to the

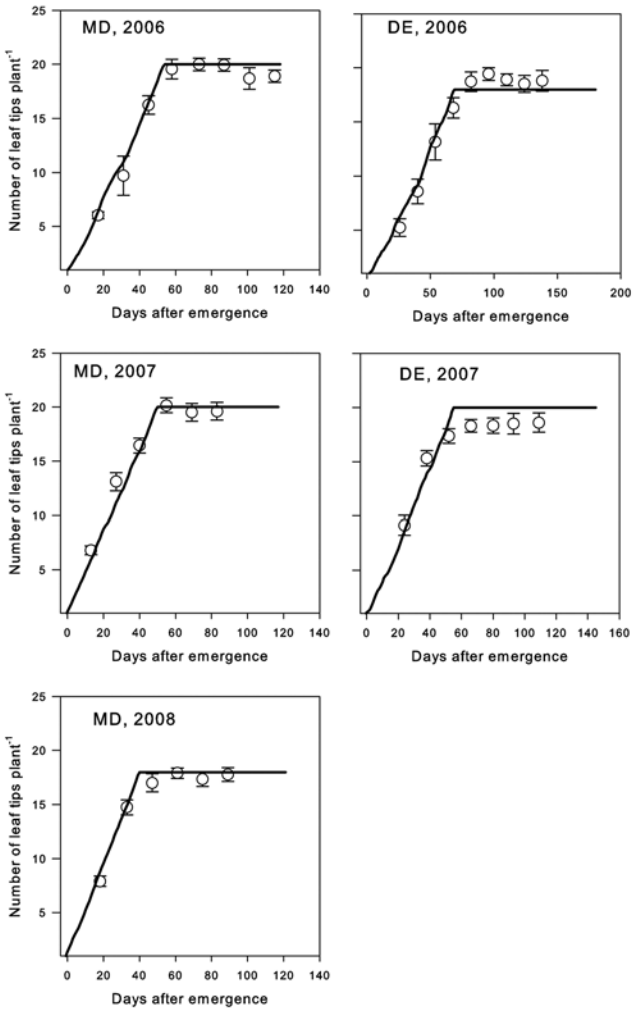

Fig. 4. Observed and simulated leaf tip number for the field data from Delaware and Maryland. The symbols represent observed data with standard errors.

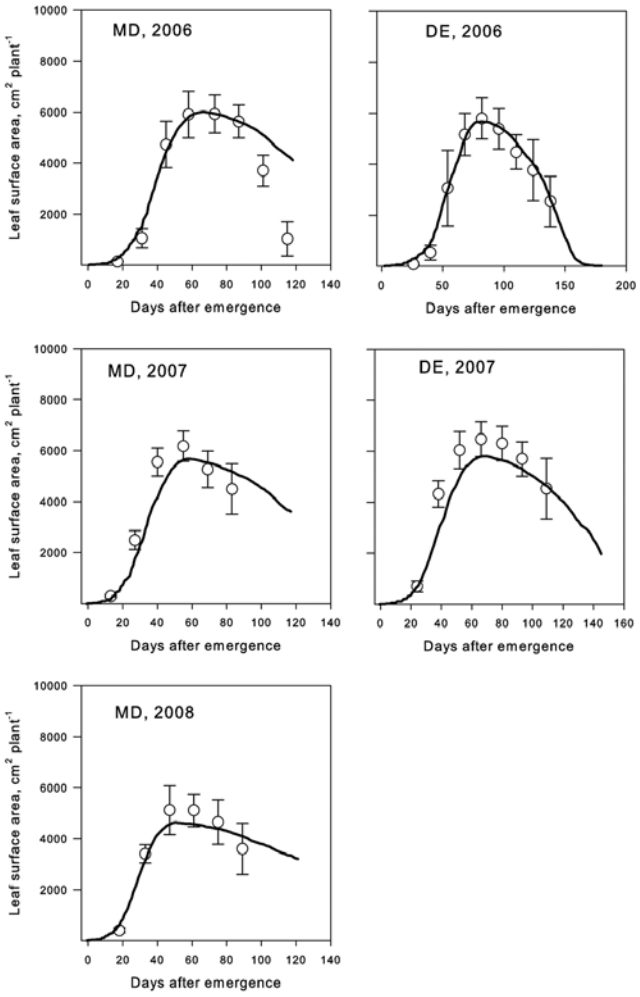

Fig. 5. Observed and simulated leaf area for the field data from Delaware and Maryland. The symbols represent observed data with standard errors.

observed values. The estimated and observed leaf areas were similar both during rapid canopy expansion and after the canopy had fully expanded. The mean error tended to vary around zero (ME in Table 3), but three of the five simulations underestimated the leaf area slightly before and at maximum leaf area. Most of the error was toward the end of the growth period when the canopy began to senesce, where the model is likely to underestimate senescence. The model tended to overestimate leaf mass on average (Fig. 6; Table 3); the RMSEs were largest for both sites in 2006. The more rapid rate of simulated leaf dry matter addition relative to the observed values contributed to the error for the Delaware 2007 data since maximum leaf weight (dead and green) estimates were close to the observed ones. The maximum observed total leaf weights were near 45 to 50 g plant^{-1} (2500–3000 kg ha^{-1}) except for those at the Maryland site in 2008, which were closer to 35 g plant^{-1} (2000 kg ha^{-1}) (Fig. 6). The simulation of dropped leaves generally underestimated the observed data (Fig. 7). This contributed to the overestimation of green leaf area toward the end of the growing season in Fig. 5 for the Maryland site.

Stem dry matter was also more likely to be overestimated than underestimated (Table 3; Fig. 8), especially the final values. The estimated values were generally close to the observed ones at the beginning of the growing season (Fig. 8) during the rapid growth phase. The differences were greatest for the final stem masses. The largest errors were for both sites in 2006, where the average bias for stem dry matter was –25.7 g plant^{-1} (1876 kg ha^{-1}) (Table 3), indicating an overestimation by the model.

In our simulations, ear dry matter accumulation (Fig. 9) began slightly earlier in some cases than did the observed dry matter accumulation. The predicted values were generally close to the observed ones, except for Maryland in 2007 where they were underestimated. The RMSE ranged from 21 to 37 g plant^{-1} (1600–2600 kg ha^{-1}). Total simulated shoot dry matter (Fig. 10) was very similar to the observed values except for 2006, when they were overestimated for both the Maryland and Delaware sites (Table 3). The consistently negative ME values in Table 3 indicate that total shoot dry matter was overestimated in all cases, i.e., the estimation error did not vary about zero. The simulated results do reflect differences in sites and years. For example, the simulated and observed dry matter at Delaware in 2006 and 2007 was higher than for the Maryland site for the same years. Delaware was planted earlier than Maryland in both years, and the Maryland site tends to be cooler because it borders the Chesapeake Bay.

Table 3. Performance evaluation results for dry matter, leaf area, and leaf appearance. Willmott's *d*, modeling efficiency (EF), mean error (ME) and root mean square error (RMSE) were calculated from Eq. [18–21].

Source	Site	Year	D	EF	ME	RMSE
Leaf area, cm^2 $plant^{-1}$	Delaware	2006	0.99	0.96	−115.9	372.6
		2007	0.95	0.82	591.9	803.8
	Maryland	2006	0.91	0.68	−608.4	1276.9
		2007	0.96	0.85	302.0	789.9
		2008	0.98	0.93	152.6	447.9
Ear weight, kg ha^{-1}	Delaware	2006	0.98	0.91	−12.3	25.3
		2007	0.98	0.95	4.6	21.8
	Maryland	2006	0.98	0.89	−19.8	26.2
		2007	0.84	0.63	13.0	28.4
		2008	0.93	0.67	−28.1	37.1
Leaf weight, kg ha^{-1}	Delaware	2006	0.93	0.75	−6.2	8.3
		2007	0.96	0.85	−4.8	5.3
	Maryland	2006	0.89	0.48	−9.6	10.3
		2007	0.95	0.75	−6.7	7.5
		2008	0.96	0.89	0.2	3.8
Shoot weight, kg ha^{-1}	Delaware	2006	0.96	0.83	−44.3	56.7
		2007	0.99	0.95	−17.9	28.5
	Maryland	2006	0.96	0.82	−48.8	56.3
		2007	0.98	0.93	−0.6	26.2
		2008	0.97	0.88	−31.1	37.5
Stem weight, kg ha^{-1}	Delaware	2006	0.91	0.53	−25.7	31.5
		2007	0.95	0.75	−17.0	21.5
	Maryland	2006	0.95	0.76	−19.5	23.3
		2007	0.98	0.93	−6.8	11.9
		2008	0.98	0.94	−3.0	10.7
Leaf tip number, no. $plant^{-1}$	Delaware	2006	0.99	0.96	0.1	1.0
		2007	0.96	0.80	−0.8	1.4
	Maryland	2006	0.99	0.97	−0.6	0.8
		2007	0.99	0.96	0.4	1.0
		2008	0.99	0.97	−0.5	0.6

The performance evaluation data (Table 3) showed that the model simulations were reasonably accurate. Most of Wilmott's *d* values were >0.9, and the lowest value was 0.84 for the Maryland 2007 ear weight. This location also had a low EF value (0.63), possibly due to large variation in the observed data. The RMSE of the shoot dry matter ranged from 26 to 56 g $plant^{-1}$ (1800–2600 kg ha^{-1}). The RMSE is about 8 to 12% of the maximum values for shoot dry matter. These are in the range of values reported by Lizaso et al. (2011) for a simulation of shoot dry matter using IXIM-Maize calibrated with observed data. Lizaso et al. (2011), however, did not show the variance in the observed data. The performance estimates for Wilmott's *d* in Table 3 were in a similar range to those given by Nendel et al. (2011) for biomass and leaf area simulations of crops grown in a Free Area Carbon Enrichment (FACE) experiment in Europe. Variability of the observed data also contributed to the error in our case because we used plot averages rather than overall site averages for the calculations. Nevertheless, most simulations fell within the range of the observed data. The negative mean errors for shoot and stem dry matter suggest that the model overestimated the masses of these components. Leaf area and ear weight, however, varied evenly above and below zero. Because crop models simulate potential growth under ideal conditions, some overestimation is not necessarily unexpected. There were no measured data for the roots; however, the root/shoot ratios at the end of the simulations varied from 0.11 to 0.26. This was a similar range as reported in a field study performed in Clarksville, MD (Anderson, 1988).

DISCUSSION

Overall, incorporation of the simplified β distribution function (Eq. [1] and [15]), a peaked exponential function (Eq. [14]), and a Q_{10} function (Eq. [16]) using hourly temperature input into a GDD-based leaf-expansion model (Lizaso et al., 2003) and phenology model (Grant, 1989a) was feasible and successful in MAIZSIM. The nonlinear temperature functions were parameterized using data from growth chamber experiments and the literature (e.g., Hesketh and Warrington, 1989; Kim et al., 2007) and produced satisfactory simulations for the maize cultivars grown in the field. The simulated leaf appearance and leaf areas for the farm sites were close to the observed data without the necessity of calibrating any parameters using the observed Maryland or Delaware data. Dry matter predictions for different plant components were also generally within the range of the observed data. Further research will be useful to examine the temperature dependence of the GDD-based leaf-expansion model parameters (i.e., ke and te from Lizaso et al. [2003] used in Eq. [2]) in more detail at the individual leaf level. The temperature dependence of ke and te used in Eq. [15] and [16] in this study was estimated from the whole-plant leaf growth data of Kim et al. (2007), which is likely to have been

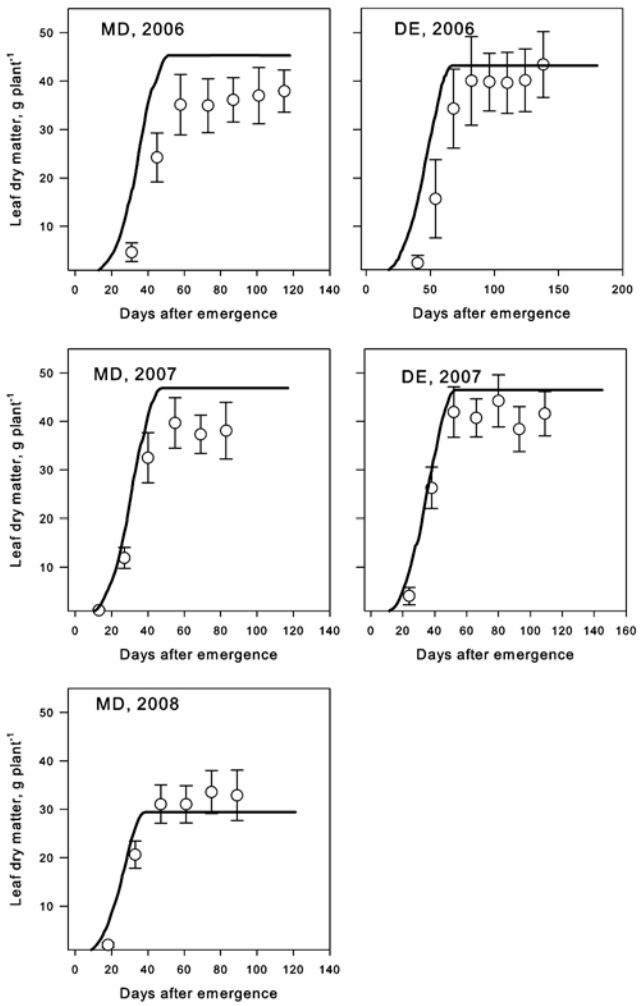

Fig. 6. Observed and simulated leaf dry matter for the field data from Delaware and Maryland. The symbols represent observed data with standard errors.

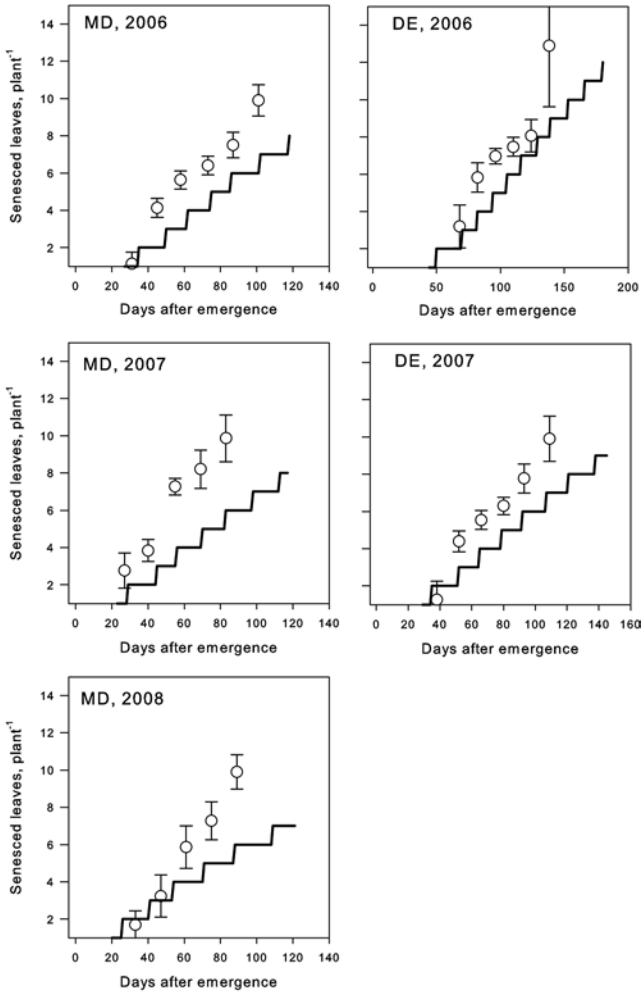

Fig. 7. Observed and simulated senesced leaf number for the field data from Delaware and Maryland. The symbols represent observed data with errors.

influenced by the growth and development of multiple leaves. Thus, direct applicability of these relationships to individual leaf growth warrants further research. On the other hand, multiple data sets from the literature support the idea that the effect of growth temperature on the potential leaf area (or leaf size) is conserved at both the individual leaf and whole-plant levels (Eq. [14]; Fig. 3a). In this work, no parameters were fit for C allocation because we used the estimates of Grant (1989b) to simulate C partitioning. The parameters for the photosynthesis model came from measurements from a portable leaf-level photosynthesis measurement system used with plants grown in SPAR chambers (Kim et al., 2006, 2007).

The use of growth chamber data proved useful to fit parameters to nonlinear rate equations (e.g., the β function) for modeling plant processes such as the leaf tip appearance rate for which the optimum occurs at high temperature. Even when using a range of planting dates in field studies, it is difficult to obtain mean air temperatures near the optimum and above (e.g., Padilla and Otegui, 2005). Thus any negative effects of supraoptimal temperatures on growth and development would be difficult to quantify in manipulated field experiments unless a wide range of locations were included (e.g., Birch et al., 1998a). On the other hand, historical yield observations in African maize trials point to a strong nonlinear decline above 30°C, resulting in 1.7% yield decline per 1°C increase under drought conditions (Lobell et al., 2011). With the increasing threat and uncertainties associated with climate change, it is imperative to develop, identify, and apply effective scientific tools (e.g., crop simulation models) that provide realistic representations of the climate impacts on food and energy security. Our model presented in this study could help address some of the limitations of traditional GDD approaches during the vegetative stage as illustrated in the literature (e.g., Bollero et al., 1996). Improving crop models for accurate simulation of temperature responses during the reproductive stage will be equally, if not more, critical for yield predictions because reproductive processes are more sensitive to high temperatures than vegetative processes in many crops including maize. Historical yield trials at multiple locations (e.g., Lobell et al., 2011), for example, can be effective resources to train and test crop models for their use in assessing climate impacts and evaluate the vulnerability and strength of various adaptive strategies. Our ability to predict crop responses to climatic conditions that are outside the historical realms using crop simulation models remains critical in adapting to climate change, particularly because many locations are expected to experience more

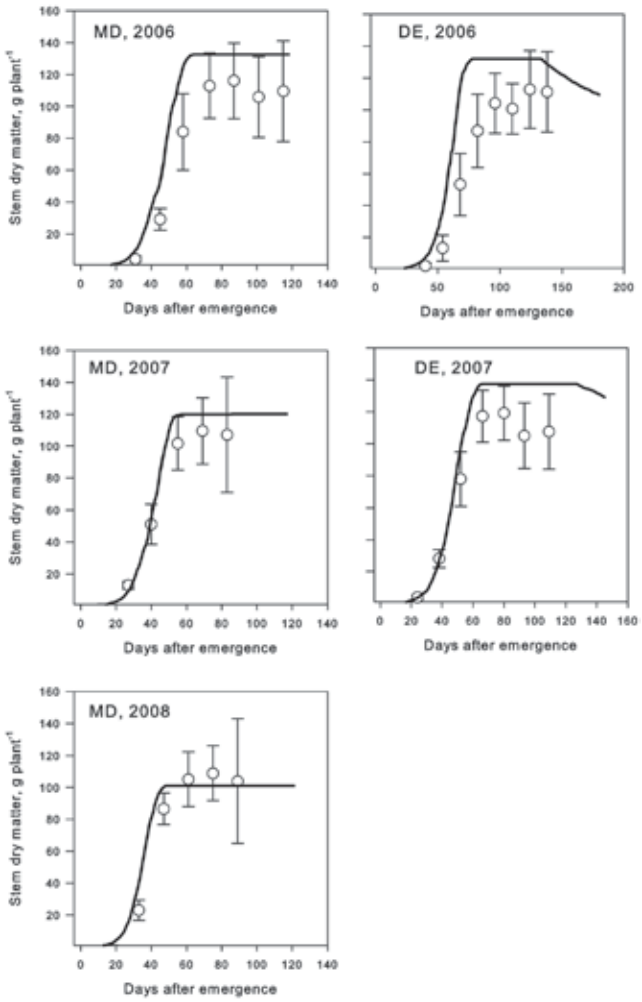

Fig. 8. Observed and simulated stem dry matter for the field data from Delaware and Maryland. The symbols represent observed data with standard errors.

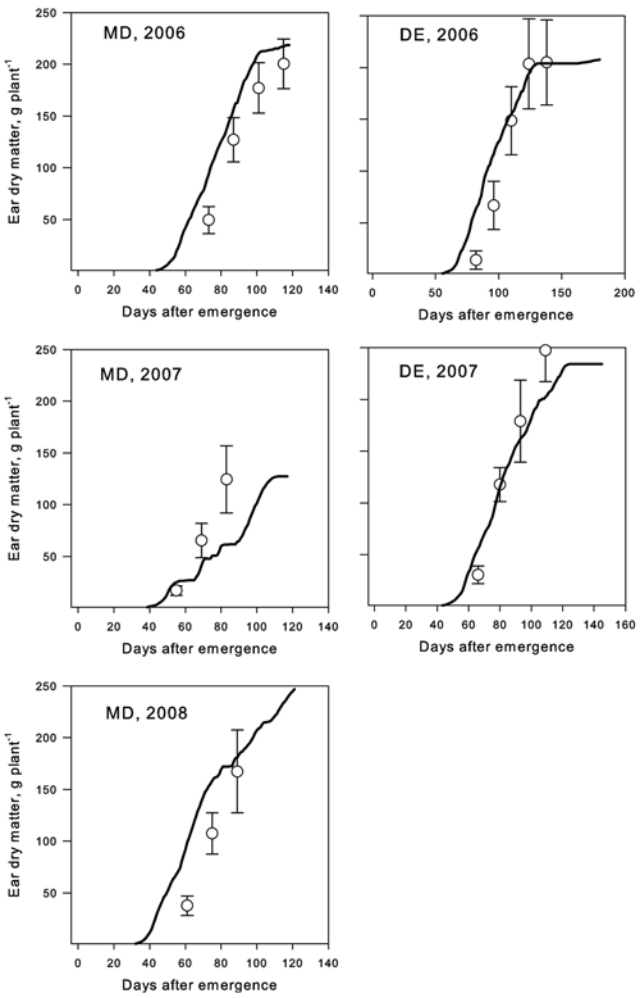

Fig. 9. Observed and simulated ear dry matter for the field data from Delaware and Maryland. The symbols represent observed data with errors.

frequent extreme temperatures under which the most current crops will become unsuitable (Battisti and Naylor, 2009).

In the present study, the differences in simulated results did not reflect differences in management other than the effect of planting date and location. The hybrids used in the field studies were similar; all required ~2600 GDD_{50F} (in °F with 50°F base temperature) to mature, corresponding to ~1700 GDD_{8C} (Table 1). The one exception was the Pioneer P37Y14 hybrid used in Maryland in 2008, which was a short-season hybrid and did not get as tall. The hybrid used for the SPAR chambers, however, was similar to the short-season hybrid used in Maryland in 2008 where it had less GDD to maturity and fewer total leaves. There were slight differences in climate between the two sites. Because the Maryland site borders on the Chesapeake Bay, the daytime ambient temperatures tend to be 2 to 3°C cooler than at the Delaware site. All the fields were fertilized with sufficient N. The more N was applied at the Delaware site than at the Maryland site because the N was applied with irrigation water. The N concentrations of the plants at all the sites, however, were near or above optimum levels (Yang et al., 2012). The Maryland site had sufficient rainfall except for 2007, when there was some water stress for a period of 14 d in mid-July. At the start of this time, about 13 to 14 leaves had emerged but the tassel was forming. There were about 10 more days of water stress during the reproductive phase. This water stress probably contributed to the differences in ear and total dry matter between the Delaware and Maryland sites in 2007. The water stress occurred after many of the leaves had emerged and expanded, thus the leaf and stem dry matter values did not vary greatly between the two sites in 2007. The maximum simulated and observed leaf areas were lowest for the 2008 Maryland site (Fig. 5). This was probably due to the late planting date (30 d later than for the 2006 and 2007 Maryland planting dates). Therefore, the model appeared to capture the effect of the late planting.

The model simulated aboveground dry matter components well but generally overestimated leaf and stem dry matter. The overestimation generally occurred at full canopy development. The simulated leaf area at full canopy was more accurate than leaf mass, suggesting that the model was not reducing C allocation to the leaves early enough. The reason for this difference, especially for stem dry matter, is at least partially related to storage of soluble C toward the end of the plant's vegetative stage. This C is stored in the stem of the plant and remobilized with time according to a valve function (Grant, 1989b). As a result, inaccurate remobilization of soluble C storage to reproductive organs may have contributed to the observed discrepancies when estimating leaf and stem biomass at the end of

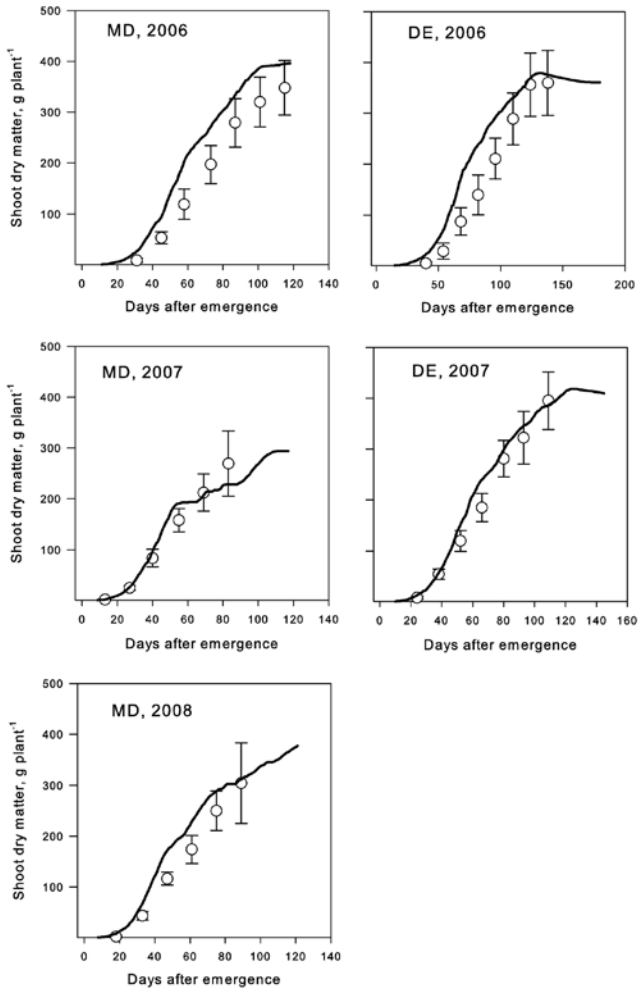

Fig. 10. Observed and simulated total shoot dry matter for the field data from Delaware and Maryland. The symbols represent observed data with standard errors.

the vegetative stage. Partitioning of C to various plant organs is difficult to accurately simulate in plant models. Our quantitative whole-plant understanding of C allocation to various plant organs has not improved greatly since Gifford and Evans (1981). As a result, C partitioning in models is still largely empirical. The method of Grant (1989b) works well because it is strongly connected to phenology, which in maize is relatively straightforward to describe.

The use of the C_4 biochemical model (von Caemmerer, 2000) gave realistic results for total dry matter simulation given that the parameters came from a portable leaf-level photosynthesis measurement system used on plants grown in SPAR chambers (Kim et al., 2006, 2007). The sunlit and shaded concept (De Pury and Farquhar, 1997) worked well for simulating canopy C gain. Overall, our results highlight the importance of simulating a realistic representation of leaf area expansion and its impact on dry matter production. The results also provide confidence in the applicability of parameters developed using growth chamber data to field conditions when the model parameters have biological meanings based on underlying processes with explanatory mechanisms.

While more tests are needed under a wide variation in environmental conditions, genotypes, and management options, our results are encouraging and suggest that data from a number of controlled-environment studies (e.g., Bos et al., 2000; Hesketh and Warrington, 1989; Kim et al., 2007; Tollenaar, 1989; Warrington and Kanemasu, 1983b) are useful to provide robust calibrations for crop models, especially under those extreme environmental conditions for which current and historical observations are lacking in field situations.

SUMMARY AND CONCLUSIONS

A set of nonlinear functions (e.g., β function, Eq. [1], and peaked exponential function, Eq. [14]) were used to describe the temperature dependence of development and growth rates for maize leaves. Existing equations describing the dependence of maize leaf canopy expansion on temperature were reformulated to use observed ambient air temperature and nonlinear function parameters to augment GDD_{8C}. The parameters for the nonlinear functions were calibrated using data from SPAR outdoor growth chambers and from other controlled-environment studies in the literature. No further field calibration was done for the model. Model simulations of leaf appearance rate, dry matter components, leaf area, and senescence were compared with observed field data at two sites during a period of 3 yr. The simulated results in a majority of the cases fell within the range of the observed data. All but one of the values of Willmott's *d* were >0.89, and the largest error in shoot dry matter was about 16%. It should be noted that the model was only tested at a limited number of locations and without significant abiotic stresses due to water, N, or temperature.

Our study provides a simple yet feasible option for improving GDD-based crop models to integrate nonlinear temperature relationships without sacrificing their current structure. In addition, our results also highlight the possibility that coupling of a more realistic representation for temperature response with the traditional GDD approach in crop models parameterized using controlled-environment data may reduce the data need for field calibration. Combined with its ability to simulate CO_2 and soil water effects, the improved temperature functions are likely to enhance the utility of MAIZSIM for assessing the impacts and risks of extreme temperatures on maize production and developing adaptive solutions to climate change. Given that the aboveground dry matter, leaf phenology, and leaf area simulations represented the observed data well, we argue that the parameters calibrated for the photosynthesis, leaf phenology, and leaf expansion models using growth chamber data were applicable to field data. This is also important from the perspective of being able to use data from controlled-environment studies to assess the climate impacts on agriculture.

ACKNOWLEDGMENT

Authors thank Jackson Fisher and Emily Morris for their assistance with growth chamber and field studies. This work was supported in part by the Specific Cooperative Agreement: 58-1265-1-074 between USDA-ARS and University of Washington.

REFERENCES

Acock, B., and V.R. Reddy. 1997. Designing an object-oriented structure for crop models. Ecol. Modell. 94:33–44. doi:10.1016/S0304-3800(96)01926-6

Acock, B., V.R. Reddy, F.D. Whisler, D.N. Baker, J.M. McKinion, H.F. Hodges, and K.J. Boote. 1982. The soybean crop simulator GLYCIM: Model documentation. PB85171163/AS. U.S. Gov. Print. Office, Washington, DC. p. 1–322.

Acock, B., and J.F. Reynolds. 1997. Introduction: Modularity in plant models. Ecol. Modell. 94:1–6. doi:10.1016/S0304-3800(96)01923-0

Ahuja, L.R., K.W. Rojas, J.D. Hanson, M.J. Shaffer, and L. Ma. 2000. Root zone water quality model: Modeling management effects on water quality and crop production. Water Resour. Publ., Highlands Ranch, CO.

Amthor, J.S. 2000. The McCree–deWit–Penning de Vries–Thornley respiration paradigms: 30 years later. Ann. Bot. 86:1–20. doi:10.1006/anbo.2000.1175

Anderson, E. 1988. Tillage and N fertilization effects on maize root growth and root:shoot ratio. Plant Soil 108:245–251. doi:10.1007/BF02375655

Arkebauer, T.J., J.M. Norman, and C.Y. Sullivan. 1995. From cell growth to leaf growth: III. Kinetics of leaf expansion. Agron. J. 87:112–121. doi:10.2134/agronj1995.00021962008700010020x

Baker, D.N., J.R. Lambert, and J.M. McKinion. 1983. GOSSYM: A simulator of cotton crop growth and yield. S. Carol. Agric. Exp. Stn. Tech. Bull. 1089. Clemson Univ, Clemson, SC.

Ball, J.T., I.E. Woodrow, and J.E. Berry. 1987. A model predicting stomatal conductance and its contribution to the control of photosynthesis under different environmental conditions. Prog. Photosynth. Res. 4:221–224.

Battisti, D.S., and R.L. Naylor. 2009. Historical warnings of future food insecurity with unprecedented seasonal heat. Science 323:240–244. doi:10.1126/science.1164363

Birch, C.J., G.L. Hammer, and K.G. Rickert. 1998a. Improved methods for predicting individual leaf area and leaf senescence in maize (*Zea mays*). Aust. J. Agric. Res. 49:249–262. doi:10.1071/A97010

Birch, C.J., J. Vos, J. Kiniry, H.J. Bos, and A. Elings. 1998b. Phyllochron responds to acclimation to temperature and irradiance in maize. Field Crops Res. 59:187–200. doi:10.1016/S0378-4290(98)00120-8

Bollero, G.A., D.G. Bullock, and S.E. Hollinger. 1996. Soil temperature and planting date effects on corn yield, leaf area, and plant development. Agron. J. 88:385–390. doi:10.2134/agronj1996.00021962008800030005x

Boote, K.J., J.W. Jones, G. Hoogenboom, and N.B. Pickering. 1998. The CROPGRO model for grain legumes. In: G. Tsuji et al., editors, Understanding options for agricultural production. Kluwer Acad. Publ., Dordrecht, the Netherlands. p. 99–128.

Boote, K.J., and N.B. Pickering. 1994. Modeling photosynthesis of row crops. HortScience 29:1423–1434.

Bos, H.J., H. Tijani-Eniola, and P.C. Struik. 2000. Morphological analysis of leaf growth of maize: Responses to temperature and light intensity. Neth. J. Agric. Sci. 48:181–198.

Brown, R.A., and N.J. Rosenberg. 1999. Climate change impacts on the potential productivity of corn and winter wheat in their primary United States growing regions. Clim. Change 41:73–107. doi:10.1023/A:1005449132633

Campbell, G.S., and J.M. Norman. 1998. An introduction to environmental biophysics. Springer, New York.

Cowan, I.R. 1965. Transport of water in the soil–plant–atmosphere system. J. Appl. Ecol. 2:221–239.

Daughtry, C.S.T., and S.E. Hollinger. 1984. Costs of measuring leaf area index of corn. Agron. J. 76:836–841. doi:10.2134/agronj1984.00021962007600050028x

De Pury, D.G.G., and G.D. Farquhar. 1997. Simple scaling of photosynthesis from leaves to canopies without the errors of big-leaf models. Plant Cell Environ. 20:537–557. doi:10.1111/j.1365-3040.1997.00094.x

Dosio, G.A., H. Rey, J. Lecoeur, N. Izquierdo, L. Aguirreza, F. Tardieu, and O. Turc. 2003. A whole-plant analysis of the dynamics of expansion of individual leaves of two sunflower hybrids. J. Exp. Bot. 54:2541–2552. doi:10.1093/jxb/erg279

Dwyer, L.M., D.W. Stewart, R.I. Hamilton, and L. Houwing. 1992. Ear position and vertical distribution of leaf area in corn. Agron. J. 84:430–438. doi:10.2134/agronj1992.00021962008400030016x

Fleisher, D.H., R.M. Shillito, D.J. Timlin, S.H. Kim, and V. Reddy. 2006. Approaches to modeling potato leaf appearance rate. Agron. J. 98:522–528. doi:10.2134/agronj2005.0136

Fleisher, D.H., and D.J. Timlin. 2006. Modeling expansion of individual leaves in the potato canopy. Agric. For. Meteorol. 139:84–93. doi:10.1016/j.agrformet.2006.06.002

Fournier, C., and B. Andrieu. 1998. A 3D architectural and process-based model of maize development. Ann. Bot. 81:233–250. doi:10.1006/anbo.1997.0549

Francis, C.A., J.N. Rutger, and A.F.E. Palmer. 1969. A rapid method for plant leaf area estimation in maize (*Zea mays* L.). Crop Sci. 9:537–539. doi:10.2135/cropsci1969.0011183X000900050005x

Gaiser, T., M. Judex, A.M. Igué, H. Paeth, and C. Hiepe. 2011. Future productivity of fallow systems in sub-Saharan Africa: Is the effect of demographic pressure and fallow reduction more significant than climate change? Agric. For. Meteorol. 151:1120–1130. doi:10.1016/j.agrformet.2011.03.015

Gifford, R.M., and L.T. Evans. 1981. Photosynthesis, carbon partitioning and yield. Annu. Rev. Plant Physiol. 32:485–509. doi:10.1146/annurev.pp.32.060181.002413

Grant, R.F. 1989a. Simulation of maize phenology. Agron. J. 81:451–457. doi:10.2134/agronj1989.00021962008100030011x

Grant, R.F. 1989b. Simulation of carbon assimilation and partitioning in maize. Agron. J. 81:563–571. doi:10.2134/agronj1989.00021962008100040004x

Hesketh, J.D., and I.J. Warrington. 1989. Corn growth response to temperature: Rate and duration of leaf emergence. Agron. J. 81:696–701. doi:10.2134/agronj1989.00021962008100040027x

Hoogenboom, G., C.H. Porter, P.W. Wilkens, K.J. Boote, L.A. Hunt, and J.W. Jones. 2010. The Decision Support System for Agrotechnology Transfer (DSSAT): Past, current and future developments. p. 50–51. In: Program and Summaries, 40th Biological Systems Simulation Conference, Maricopa, AZ. 13–15 Apr. 2010. USDA-ARS Arid-Land Agric. Res. Ctr., Maricopa, AZ.

Iqbal, M.A., J. Eitzinger, H. Formayer, A. Hassan, and L.K. Heng. 2011. A simulation study for assessing yield optimization and potential for water reduction for summer-sown maize under different climate change scenarios. J. Agric. Sci. 149:129–143. doi:10.1017/S0021859610001243

Jones, C.A., and J.R. Kiniry. 1986. CERES-Maize: A simulation model of maize growth and development. Texas A&M Univ. Press, College Station.

Jones, J.W., G. Hoogenboom, C.H. Porter, K.J. Boote, W.D. Batchelor, L.A. Hunt, et al. 2003. The DSSAT cropping system model. Eur. J. Agron. 18:235–265. doi:10.1016/S1161-0301(02)00107-7

Keating, B.A., P.S. Carberry, G.L. Hammer, M.E. Probert, M.J. Robertson, D. Holzworth, et al. 2003. An overview of APSIM, a model designed for farming systems simulation. Eur. J. Agron. 18:267–288. doi:10.1016/S1161-0301(02)00108-9

Kim, S.-H., D.C. Gitz, R.C. Sicher, J.T. Baker, D.J. Timlin, and V.R. Reddy. 2007. Temperature dependence of growth, development, and photosynthesis in maize under elevated CO_2. Environ. Exp. Bot. 61:224–236. doi:10.1016/j.envexpbot.2007.06.005

Kim, S.-H., and J.H. Lieth. 2003. A coupled model of photosynthesis, stomatal conductance and transpiration for a rose leaf (*Rosa hybrida* L.). Ann. Bot. 91:771–781. doi:10.1093/aob/mcg080

Kim, S.-H., R.C. Sicher, H. Bae, D.C. Gitz, J.T. Baker, D.J. Timlin, and V.R. Reddy. 2006. Canopy photosynthesis, evapotranspiration, leaf nitrogen, and transcription profiles of maize in response to CO_2 enrichment. Global Change Biol. 12:588–600. doi:10.1111/j.1365-2486.2006.01110.x

Lafarge, T., and F. Tardieu. 2002. A model co-ordinating the elongation of all leaves of a sorghum cultivar was applied to both Mediterranean and Sahelian conditions. J. Exp. Bot. 53:715–725. doi:10.1093/jexbot/53.369.715

Lambert, J.R., and D.N. Baker. 1984. RHIZOS: A simulation of root growth and soil processes: I. Model description. S. Carol. Agric. Exp. Stn. Tech. Bull. 1080. Clemson Univ., Clemson, SC.

Lizaso, J.I., W.D. Batchelor, K.J. Boote, and M.E. Westgate. 2005. Development of a leaf-level canopy assimilation model for CERES-Maize. Agron. J. 97:722–733. doi:10.2134/agronj2004.0171

Lizaso, J.I., W.D. Batchelor, and M.E. Westgate. 2003. A leaf area model to simulate cultivar-specific expansion and senescence of maize leaves. Field Crops Res. 80:1–17. doi:10.1016/S0378-4290(02)00151-X

Lizaso, J.I., K.J. Boote, J.W. Jones, C.H. Porter, L. Echarte, M.E. Westgate, and G. Sonohat. 2011. CSM-IXIM: A new maize simulation model for DSSAT version 4.5. Agron. J. 103:766–779. doi:10.2134/agronj2010.0423

Lobell, D.B., M. Banziger, C. Magorokosho, and B. Vivek. 2011. Nonlinear heat effects on African maize as evidenced by historical yield trials. Nat. Clim. Change 1:42–45. doi:10.1038/nclimate1043

Loomis, R.S., and D.J. Connor. 1996. Crop ecology: Productivity and management in agricultural systems. Cambridge Univ. Press, New York.

Muchow, R.C., T.R. Sinclair, and J.M. Bennett. 1990. Temperature and solar radiation effects on potential maize yield across locations. Agron. J. 82:338–343. doi:10.2134/agronj1990.00021962008200020033x

Nendel, C., M. Berg, K.C. Kersebaum, W. Mirschel, X. Specka, M. Wegehenkel, et al. 2011. The MONICA model: Testing predictability for crop growth, soil moisture and nitrogen dynamics. Ecol. Modell. 222:1614–1625. doi:10.1016/j.ecolmodel.2011.02.018

Padilla, J.M., and M.E. Otegui. 2005. Co-ordination between leaf initiation and leaf appearance in field-grown maize (*Zea mays*): Genotypic differences in response of rates to temperature. Ann. Bot. 96:997–1007. doi:10.1093/aob/mci251

Pearce, R.B., J.J. Mock, and T.B. Bailey. 1975. Rapid method for estimating leaf area per plant in maize. Crop Sci. 15:691–694. doi:10.2135/cropsci1975.0011183X001500050023x

Reid, J.F., B. Zur, and J.D. Hesketh. 1990. The dynamics of a maize canopy development: 2. Leaf area growth. Biotronics 19:99–107.

Reynolds, J.F., and B. Acock. 1997. Modularity and genericness in plant and ecosystem models. Ecol. Modell. 94:7–16. doi:10.1016/S0304-3800(96)01924-2

Stewart, D.W., L.M. Dwyer, and L.L. Carrigan. 1998. Phenological temperature response of maize. Agron. J. 90:73–79. doi:10.2134/agronj1998.00021962009000010014x

Stockle, C.O., P.T. Dyke, J.R. Williams, C.A. Jones, and N.J. Rosenberg. 1992. A method for estimating the direct and climatic effects of rising atmospheric carbon dioxide on growth and yield of crops: II. Sensitivity analysis at three sites in the midwestern USA. Agric. Syst. 38:239–256. doi:10.1016/0308-521X(92)90068-Y

Tardieu, F., C. Granier, and B. Muller. 1999. Modelling leaf expansion in a fluctuating environment: Are changes in specific leaf area a consequence of changes in expansion rate? New Phytol. 143:33–43. doi:10.1046/j.1469-8137.1999.00433.x

Timlin, D.J., Y.A. Pachepsky, and B. Acock. 1996. A design for a modular, generic soil simulator to interface with plant models. Agron. J. 88:162–169. doi:10.2134/agronj1996.00021962008800020008x

Timlin, D.J., Ya. Pachepsky, B.A. Acock, J. Šimunek, G. Flerchinger, and F. Whisler. 2002. Error analysis of soil temperature simulations using measured and estimated hourly weather data with 2DSOIL. Agric. Syst. 72:215–239. doi:10.1016/S0308-521X(01)00075-0

Tollenaar, M. 1989. Response of dry matter accumulation in maize to temperature: I. Dry matter partitioning. Crop Sci. 29:1239–1246. doi:10.2135/cropsci1989.0011183X002900050030x

Tuzet, A., A. Perrier, and R. Leuning. 2003. A coupled model of stomatal conductance, photosynthesis and transpiration. Plant Cell Environ. 26:1097–1116. doi:10.1046/j.1365-3040.2003.01035.x

van Genuchten, M.Th. 1980. A closed-form equation for predicting the hydraulic conductivity of unsaturated soils. Soil Sci. Soc. Am. J. 44:892–898. doi:10.2136/sssaj1980.03615995004400050002x

van Ittersum, M.K., P.A. Leffelaar, H. van Keulen, M.J. Kropff, L. Bastiaans, and J. Goudriaan. 2003. On approaches and applications of the Wageningen crop models. Eur. J. Agron. 18:201–234. doi:10.1016/S1161-0301(02)00106-5

von Caemmerer, S. 2000. Biochemical models of leaf photosynthesis. CSIRO Publ., Collingwood, VIC, Australia.

Warrington, I.J., and E.T. Kanemasu. 1983a. Corn growth response to temperature and photoperiod: I. Seedling emergence, tassel initiation, and anthesis. Agron. J. 75:749–754. doi:10.2134/agronj1983.00021962007500050008x

Warrington, I.J., and E.T. Kanemasu. 1983b. Corn growth response to temperature and photoperiod: II. Leaf-initiation and leaf-appearance rates. Agron. J. 75:755–761. doi:10.2134/agronj1983.00021962007500050009x

Whisler, F.D., B. Acock, D.N. Baker, R.E. Fye, H.F. Hodges, J.R. Lambert, et al. 1987. Crop simulation models in agronomic systems. Adv. Agron. 40:141–208. doi:10.1016/S0065-2113(08)60282-5

Williams, J.R. 1995. The EPIC model. In: V.P. Singh, editor, Computer models of watershed hydrology. Water Resour. Publ., Highlands Ranch, CO. p. 909–1000.

Willmott, C.J. 1981. On the validation of models. Phys. Geogr. 2:184–194.

Willmott, C.J., S.G. Ackleson, R.E. Davis, J.J. Feddema, K.M. Klink, D.R. Legates, et al. 1985. Statistics for the evaluation and comparison of models. J. Geophys. Res. 90:8995–9005. doi:10.1029/JC090iC05p08995

Yan, W., and L.A. Hunt. 1999. An equation for modelling the temperature response of plants using only the cardinal temperatures. Ann. Bot. 84:607–614. doi:10.1006/anbo.1999.0955

Yang, H., A. Dobermann, J.L. Lindquist, D.T. Walters, T.J. Arkebauer, and K.G. Cassman. 2004. Hybrid-maize—A maize simulation model that combines two crop modeling approaches. Field Crops Res. 87:131–215. doi:10.1016/j.fcr.2003.10.003

Yang, Y., D.J. Timlin, D.H. Fleisher, S.B. Lokhande, J.-A. Chun, S.-H. Kim, et al. 2012. Nitrogen concentration and dry-matter accumulation in maize crop: Assessing maize nitrogen status with an allometric function and a chlorophyll meter. Commun. Soil Sci. Plant Anal. 43:1563–1575. doi:10.1080/00103624.2012.675393

Yang, Y., S.-H. Kim, D.J. Timlin, D.H. Fleisher, B. Quebedeaux, and V.R. Reddy. 2009a. Simulating canopy transpiration and photosynthesis of corn plants under different water status using a coupled model. Trans. ASABE 52:1011–1024.

Yang, Y., D.J. Timlin, D.H. Fleisher, S.-H. Kim, B. Quebedeaux, and V.R. Reddy. 2009b. Simulating leaf area of corn plants at contrasting water status. Agric. For. Meteorol. 149:1161–1167. doi:10.1016/j.agrformet.2009.02.005

Yin, X., J. Goudriaan, E. Lantinga, J. Vos, and H. Spiertz. 2003. A flexible sigmoid function of determinate growth. Ann. Bot. 91:361–371. doi:10.1093/aob/mcg029

Yin, X., and M.J. Kropff. 1996. Use of the Beta function to quantify effects of photoperiod on flowering and leaf number in rice. Agric. For. Meteorol. 81:217–228. doi:10.1016/0168-1923(95)02324-0

Yin, X., M.J. Kropff, G. McLaren, and R.M. Visperas. 1995. A nonlinear model for crop development as a function of temperature. Agric. For. Meteorol. 77:1–16. doi:10.1016/0168-1923(95)02236-Q